




Human red blood cell membrane stiffness: why should we study it and how?

Rekha Selvan¹ and Sarbari Bhattacharya^{2,a} 

¹ Department of Science and Humanities, PES University, Ring Road Campus, Bengaluru, Karnataka 560085, India

² Department of Physics, Bangalore University, Jnanabharathi Campus, Bengaluru, Karnataka 560056, India

Received 15 November 2023 / Accepted 22 January 2024

© The Author(s), under exclusive licence to EDP Sciences, Springer-Verlag GmbH Germany, part of Springer Nature 2024

Abstract The primary function of the human red blood cells (RBCs) is to transport oxygen to all tissues in the human body for the process of cellular respiration. To do this, RBCs often need to pass through capillaries in the human vasculature which have diameters smaller than that of the RBC, requiring them to undergo extensive deformations. An altered RBC cell membrane stiffness (CMS), thereby, is likely to have consequences on the RBC flow rate. RBC CMS is known to be affected by several commonly encountered disease conditions. This mini-review gives an overview of the basic knowledge needed to study RBC transport in microcirculation and outlines the various techniques utilized to measure the RBC CMS. It also describes in detail certain techniques that are best suited to further understanding of in vivo RBC microcirculation.

1 Introduction

All aerobic organisms require molecular oxygen for the processes of mitochondrial respiration and oxidative phosphorylation at the cellular level. In vertebrates, it is transported to the tissues through closed circulation of blood via the cardiovascular system. Human blood consists of plasma, red blood cells (RBCs), white blood cells (WBCs), and platelets, with RBCs forming the major cellular component [1]. The cytoplasm in the RBCs is rich in an iron containing complex metalloprotein called hemoglobin that is capable of temporarily binding to oxygen. About 98% of the total oxygen is transported in the blood, reversibly bound to the hemoglobin present in the RBCs, while the other 2% is transported dissolved in the plasma and RBC water [2]. The viscoelastic properties of the RBCs, thereby, are of extreme importance as they repeatedly squeeze through capillaries in the circulatory system with diameters much smaller than their own, without any compromise on their functionality. The average circulation time of an RBC is said to be about 60 s [3] and the average lifespan of the RBC is approximately 120 days [1] which would amount to a very large number of such extensive deformations. Alterations in the viscoelastic properties of the RBC thereby are bound to have consequences in terms of the rate of nutrient and oxygen supply to the tissues.

It is well known that medical conditions like hyperglycemia [4], jaundice [5], malaria [6], and sickle cell disease [7] increase the cell membrane stiffness (CMS) of RBCs. It is thereby imperative to study the effect of this altered RBC CMS on the RBC microcirculation. An altered rate of oxygen and nutrient supply to tissues could be correlated with the various symptoms and complications that are associated with these medical conditions. Establishing a proper cause-and-effect chronology here could help in early diagnostics and improve the likelihood of a more effective treatment.

This review, starting from a basic description of the RBC structure and the circulatory system through which it is transported along with the analytical models developed to understand it, gives an overview of a wide variety of tools and methods that are used to estimate the viscoelastic properties of RBCs. As the stress regimes involved in these methods are extremely different, the conclusions with regards to the viscoelastic response of the RBC is varied depending on the exact technique utilized. Thus, though all these techniques, in principle, provide a measure of the RBC CMS, not all of these are suited to understand the effects of altered RBC CMS on microcirculation. The review further describes, in some detail, certain techniques that employ stress regimes close to that experienced by

^a e-mail: sarbari.bhattacharya@bub.ernet.in (corresponding author)

RBCs in microcirculation and thereby yield results that are best suited to understand RBC dynamics in narrow passages under conditions encountered in human vasculature.

2 Human red blood cells

Human blood consists of plasma and cellular components. Plasma is 92% water, 7% proteins like albumin, globulins, and fibrinogen with the remaining 1% being made up of electrolytes, dissolved gases, nutrients, and metabolic wastes [8, 9]. The viscosity of plasma is about 0.0012 Pa.s at 37 °C [10]. RBCs, the major cellular component, have a hematocrit value (ratio of red blood cell volume to the total volume of blood) of approximately 40–45% (4.8–5.4 million cells per microliter) [11]. RBCs can be described as bi-concave disks with diameter in the range 6.2–8.2 μm and thickness that changes along a diametrical line from about 1 μm at the center (dimple region) to a maximum of about 2 μm close to the edge (rim). The surface area and volume of RBC are approximately 130–140 μm^2 and 90–110 fl, respectively [1]. The surface area of the RBC is in excess of what is required to cover the volume of RBC. This excess surface area helps the RBC in undergoing large deformations without rupturing while passing through narrow blood channels during their life span. A pH of 7.4 is required for normal functioning of RBCs [1].

2.1 Functions of RBCs

As stated earlier, the most important function of the RBC is to carry oxygen and nutrients to different parts of the body and that the oxygen transport happens primarily because of the hemoglobin contained in the RBCs. Hemoglobin is made up of four protein subunits (globin) and embedded within each of these globular proteins is a heme group containing an Fe^{2+} ion which can bind one O_2 molecule. Thus, each hemoglobin molecule can carry 4 oxygen molecules. This oxygen is then transported to various tissues in the body through a huge network of blood vessels [8]. About 80% of the carbon dioxide that is an end product of metabolism in the tissues is carried as bicarbonate in the water content of the RBC, while 10% binds to hemoglobin (and other proteins) forming carbaminohemoglobin and is transported to the lungs where it is removed from the body by expiration. Participation in the CO_2 level regulation in the body gives the RBC a role in maintaining the pH of the blood. RBCs have also been found to be involved in functions like controlling bio-availability of nitric oxide required for proper vascular functioning [12], redox regulation, and blood rheology [13]. It has been shown that the RBC also expresses several adhesion molecules on its membrane surface [14].

2.2 Life cycle of RBC

RBCs are produced in the bone marrow at the rate of 2 million cells per second [8] using amino acids, glucose, lipids, iron, copper, zinc, and other elements. Young RBCs (reticulocytes) consist of a few cell organelles which they lose once they are in circulation. Mature RBCs (erythrocytes) lack nucleus, mitochondria, and endoplasmic reticulum. They obtain energy by converting glucose anaerobically into adenosine triphosphate (ATP) [15]. Erythrocytes have a life span of approximately 120 days, as stated earlier, and travel more than 300 km during this time [16]. As they age, RBCs lose surface area and deformability. RBCs that are unable to change shape to suit circulation conditions, like damaged and old RBCs (senescent RBCs), are trapped in the spleen and destroyed (hemolysis). Damaged RBCs are removed by macrophages while passing through liver, spleen, and bone marrow [17–19].

2.3 Structure of RBC

RBC structure consists of cytoplasm with dissolved proteins and a cell membrane consisting of cytoskeleton (on the cytosol side) and plasma membrane (on the outer side).

Cytoplasm The cytoplasm of the RBC is a dense aqueous mixture of hemoglobin and other proteins. A single RBC can contain more than 300 million hemoglobin molecules. The cytoplasmic viscosity (6.07 ± 3.8 mPa.s) is higher than that of the blood plasma due to the presence of haemoglobin [20]. The physiological osmolarity of blood plasma is found to be 295 mOsm/kg [21] which is nothing but the osmolarity of the RBC cytoplasm. Any variation in the osmolarity leads to shape changes of RBC.

Cytoskeleton RBC cytoskeleton is a two-dimensional sheet like structure with dynamic linkages. It consists of a triangular network of peripheral membrane proteins like spectrin, ankyrin, and band 4.1 as well as transmembrane proteins like band 3 and glycophorin C. It can extend into the cytoplasm up to 50 nm. Spectrin is a twisted heterodimer protein with α and β subunits [22]. Six spectrin tetramers are linked to one actin molecule through band 4.1 molecules. This protein complex junction is then anchored to a membrane protein glycophorin C through

six band 4.1 molecules (Fig. 1). These protein complex junctions can move freely to make any conformational changes, thus providing deformability to the RBC membrane. Additionally, one ankyrin molecule binds at the middle of each spectrin tetramer and is directly linked to a band 3 tetramer of the plasma membrane [1]. The cytoskeleton helps in stabilizing the RBC shape against any asymmetric changes in the composition of plasma membrane [23] and offers mechanical resistance. Spectrin and proteins that attach the spectrin lattice to the bilayer play an important role in determining the deformability of RBCs.

Plasma membrane Plasma membrane is a double-tailed lipid bilayer, with a few proteins, in L- α fluid phase. It is about 4 nm thick. It is a quasi-2D structure that is anchored to the cytoskeleton at specific sites. Around 60% of the RBC membrane is made up of phospholipids [1], while 13% is constituted by other phospholipidic minor components. About 23% of lipid bilayer consists of cholesterol. At pH of 7.4, most of the phospholipids are neutral except for phosphatidylserine, phosphatidic acid, and phosphatidylinositol. The lipids are asymmetrically distributed between the inner and outer lipid layers [25], essential for maintaining the bi-concave shape of RBC.

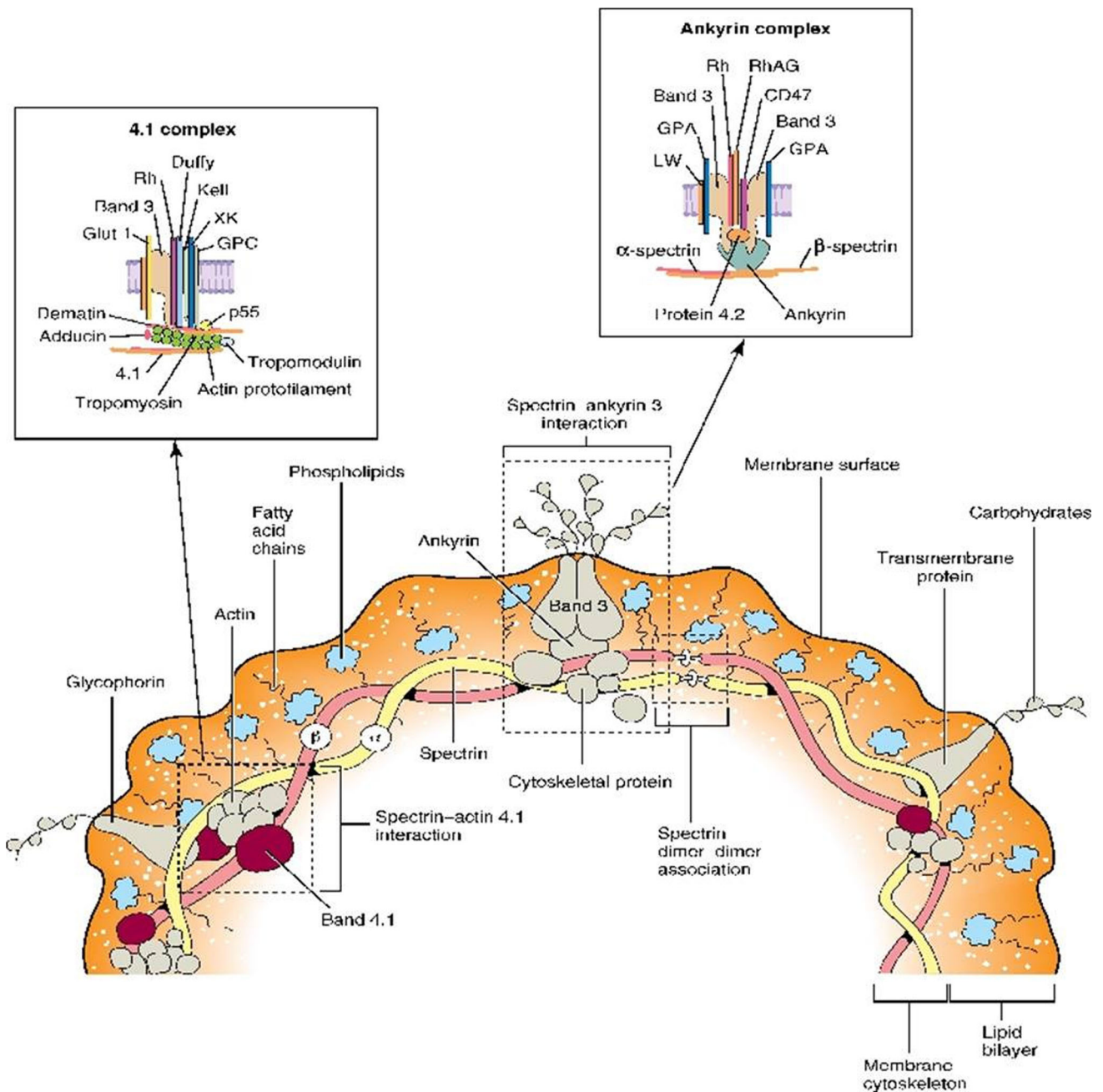


Fig. 1 Structure of RBC membrane [24]. Printed with permission from Elsevier

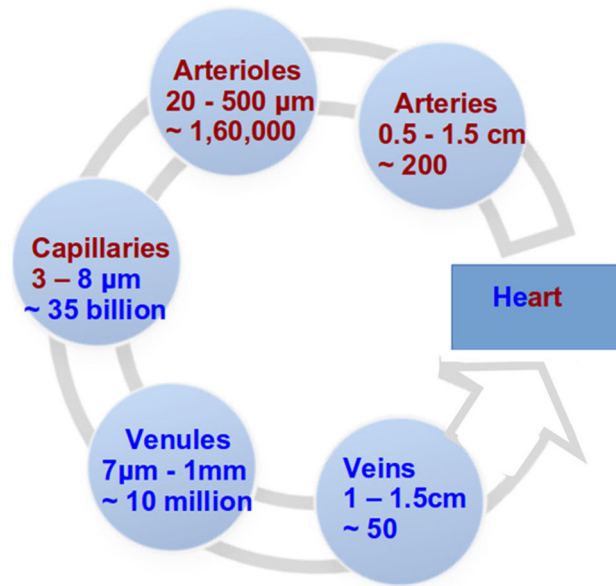


Fig. 2 Different blood vessels encountered in human vasculature along with their typical diameters and numbers. Red: oxygenated blood and blue: deoxygenated blood

RBC membrane fluidity exclusively depends on the composition of lipids, degree of extent of saturation of fatty acids, and cholesterol content [14]. Being in a fluid phase, the plasma membrane can be easily deformed.

It is evident that the RBC shape and deformability is mainly controlled by the cytoskeletal membrane proteins and plasma membrane lipids. Any changes in these will lead to an altered deformability/cell membrane stiffness (CMS) of RBCs. The composite membrane made of the cytoskeleton (elastic) and plasma membrane (viscous) along with the cytoplasm (viscous) makes the RBC a viscoelastic structure.

3 Circulation of blood through human vasculature

The blood in the human body is constantly transported from the heart to various parts of the body and back to the heart via systemic circulation through five different types of blood vessels, namely, arteries, arterioles, capillaries, veins, and venules. It is a closed circulatory system. The number and diameter of these blood vessels found in the human body are shown in Fig. 2. At any given time, about 64% of blood is contained in veins and venules, 13% in arteries and arterioles, 7% in capillaries, 7% in the chambers of heart, and the remaining in pulmonary circulation. The blood flow rate is least in the capillaries. The flow of blood through the capillaries is referred to as microcirculation. The exchange of gases, nutrients, and wastes between blood and interstitial fluid takes place here.

4 Hemodynamics

Blood is a non Newtonian fluid. Its viscosity depends on the shear stress applied as well as the duration of application of stress [26]. At the physiological temperature of 37°C, blood is both a shear thinning as well as a thixotropic fluid [10]. At high shear rates (100–1500s⁻¹), RBCs deform rendering a low viscosity of about 2–3 cP, whereas at low shear rates (< 10s⁻¹), RBCs aggregate with each other to form rouleaux (stacked coin like structures) and increase viscosity up to 10 cP. The viscosity of the blood according to the Carreau–Yasuda model [27] is given as

$$\eta_a = \eta_\infty + (\eta_o - \eta_\infty)(1 + (\lambda\dot{\gamma})^2)^{\frac{n-1}{2}}, \quad (1)$$

with η_∞ = viscosity at infinite shear limit (0.0035 Pa.s), η_o = zero shear limit viscosity (0.056 Pa.s), n = power law index (0.36), and λ = relaxation time constant (3.313s) [28].

In larger vessels, where the shear rate is above $100s^{-1}$, blood exhibits Newtonian behavior with the viscosity value reaching a value of η_∞ [29]. In large arteries, continuum hypothesis can be used to study the flow. The flow field in large arteries is best described using the Eulerian approach with the general Navier–Stokes equation. An important dimensionless quantity that helps in the prediction of flow patterns in fluid mechanics is the Reynold’s number (Re), which is just the ratio of inertial to viscous forces. For a fluid of density ρ and viscosity η at velocity V in a pipe of hydraulic diameter L , the Reynold’s number is given as

$$Re = \frac{\rho VL}{\eta}. \tag{2}$$

Fluid flow is laminar in nature for values of $Re < 2300$, while it is turbulent for $Re > 4000$ and transient at intermediate values. Blood flows in vivo with $Re = 1$ in the smallest arterioles to 4000 in the aorta [30]. Blood vessels far from the heart can be approximated to be rigid [30]. Hydrodynamics of RBCs in narrow channels can be explained by lubrication theory.

Lubrication theory Lubrication theory has been developed to obtain relevant hydrodynamic parameters such as drag and pressure drop in the kinds of flows encountered in capillaries [31]. If a particle of radius b is passing through a channel of radius a , then Lubrication theory is applicable for case where $b/a > 0.9$. Lubrication theory assumes the following:

- The gap between the particle and the channel wall is small compared to the thickness of the particle and
- The radial velocity is small compared to the axial velocity of the fluid (V_z) (see Fig. 3).

Under steady-state laminar flow conditions along with these assumptions, the Navier–Stokes equation in cylindrical coordinates (r, θ, z) (fixed with respect to the channel wall)

$$\frac{1}{\eta} \frac{dp}{dz} = \frac{\partial^2 V_z}{\partial r^2} + \frac{1}{r} \frac{\partial V_z}{\partial r} \tag{3}$$

and

$$Q = \int_0^a 2\pi r V_z dr = \text{constant}, \tag{4}$$

where p is the pressure and Q is the volumetric flow rate including the particles.

The particles are assumed to be axi symmetric and are treated as stacks of coins of infinitesimal thickness of variable radius (Fig. 3). The solutions to the equations are obtained in two parts by assigning appropriate boundary conditions to reflect the cases where (i) $Q = 0$ and $U \neq 0$ where U is the particle velocity, representing a stream of particles moving in a fluid that is at rest and (ii) $Q \neq 0$ and $U=0$ representing stationary particles in fluid flow. The solution for V_z in both cases is obtained [31]. The drag force (D) acting on each coin is due to the shear stress (τ) acting on it at $r=R'_o$ and due to the pressure drop across the faces of the coins

$$D = 4\pi R_o'^2 \tau(r, z)_{r=R'_o} + 2\pi R_o'^3 \frac{\partial p}{\partial z}. \tag{5}$$

Drag coefficients D_U and D_V can be obtained using the solutions obtained with appropriate boundary conditions for the two cases mentioned above. The overall drag then can be written in terms of normalized drag coefficients

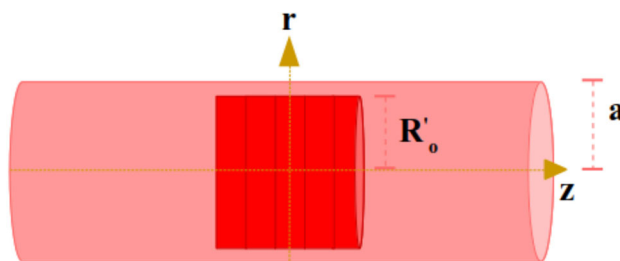


Fig. 3 Stacked coins model used in lubrication theory

Table 1 Medical conditions affecting RBC CMS

Medical condition	Effect on RBC	Studies
Hyperglycemia	Lipid peroxidation and glycosylated hemoglobin	[4, 35–39]
Jaundice	Increased bilirubin affects hemoglobin and RBC aggregation properties	[5]
Malaria	Hemoglobin degrades and new proteins transported due to invasion of parasites	[6, 40]
Sickle Cell Disease	Impaired hemoglobin leading to sickle shaped RBCs	[7, 41]
Hereditary spherocytosis	Mutations in transmembrane proteins leading to reduced S/V ratio of 1.08	[16, 42]
Elliptocytosis	Mutations in the integral RBC membrane protein	[23]
Hypertension	Reduced deformability	[43]
Covid-19	Morphological changes and increased oxidative stress	[44, 45]

K_U and K_V as follows:

$$D = 6\pi\eta b(-K_U U + K_V V). \quad (6)$$

For a Stokes flow, $K_U = K_V = 1$. The effects of gap between channel wall and particle, distance between the neighboring particles, and the shape of particles are all contained in the K_U and K_V values. The normalized drag coefficients are obtained using the equations

$$K_U = \frac{-1}{3b_0} \int_{-a_0}^{a_0} \frac{1 + R_0(z)^2}{1 - R_0(z)^2 + (1 + R_0(z)^2)\ln R_0(z)} dz \quad (7)$$

$$K_V = \frac{-1}{3b_0} \int_{-a_0}^{a_0} \frac{1}{1 - R_0(z)^2 + (1 + R_0(z)^2)\ln R_0(z)} dz; \quad (8)$$

K_U and K_V can be in general obtained for any axisymmetric particle extending from $z = -a_0$ to $+a_0$ using an appropriate shape factor $R_0(z)$. In the case of an RBC moving through a microchannel, the integration is done over the length of the shape the RBC has deformed into, to pass through the channel.

5 Enhancement of RBC membrane stiffness

The deformability of RBCs plays a vital role in microcirculation. The membrane stiffness of RBCs is found to be altered in several medical conditions [32–34]. Some of these are listed in Table 1.

There can be several conditions prevailing simultaneously in an individual that affect the RBC CMS. It is thereby not possible to draw any conclusions about comparative medical status with respect to a particular condition only by comparing the RBC CMS of two individuals. Consequently, it is not advisable to utilize RBCs extracted from different individuals when designing a new method of RBC CMS measurement or when calibrating a known technique. It is useful to know artificial means of varying the CMS of RBCs extracted from a single healthy individual in a controlled manner for utilization for such purposes. A few such methods are listed below.

A detailed investigation on the alteration of RBC CMS using BSA has been carried out [55] and is discussed in the latter part of the review.

6 Methods to study the mechanical properties of RBCs

A variety of techniques, utilizing a wide range of stress regimes and throughputs, to study RBC CMS, have been extensively reported in literature.

- **Micropipette aspiration** It was the very first technique used to measure mechanical properties of single cells. In this technique, a cell is aspirated into a pipette of suitable radius, and as the suction pressure is increased,

Table 2 Artificial means of stiffening the RBC CMS

Stiffening method	Effect on RBC	Studies
Diamide treatment	Stiffens cytoskeletal proteins by creating disulfide bonds on spectrin proteins	[41, 46, 47].
Glutaraldehyde treatment (0.02 to 0.08%w/v)	Stiffens entire cell by cross-linking cytoskeletal proteins, phospholipids in lipid bilayer and cytoplasm	[48–52]
BSA treatment	replacement of human serum proteins on certain sites of the membrane and removal of lipids from outer layer of lipid bilayer	[23, 53–55]
Heat treatment (48–50° C)	irreversible denaturation of membrane proteins	[51, 56]

the protruded length of the cell is monitored using a microscope. Micropipette aspiration has been extensively used to measure the deformability of RBCs [57–59]. The membrane bending modulus of RBCs was measured (1.8×10^{-19} Nm) from buckling measurements of RBCs in the micropipette aspiration technique [58].

- **Optical tweezers** It is a technique used to hold and manipulate microscopic particles/cells using tightly focused laser beams, exerting forces of the order of a few pN. A relatively less complicated way of assessing the viscoelastic response of the RBC is to use a dual beam optical trap to trap the RBC at diametric opposite ends (without attaching any beads) and then stretch the RBC by moving one trap, while the other is kept stationary [60, 61]. Reorientation dynamics of RBCs in optical tweezers is another method of studying the deformability of RBCs [38]. Corner frequencies extracted from Power Spectral Density analysis of RBCs in optical traps have also been used to assess its deformability [62].
- **Optical stretcher** Two non-focused identical laser beams with Gaussian intensity profile propagating in opposite directions can also be used to trap an object if the force is restoring in nature and at the center of gravity of the object, there exists no net force [63, 64]. If a deformable cell is trapped, the surface forces due to scattering of light are enough to stretch the cells in the beam direction.
- **Membrane fluctuations** The fluctuations of the cell membrane of an RBC are monitored by recording the scattered intensity of light from the edge of the rim region based on point dark-field microscopy and used to gauge the membrane bending properties [65]. Using interference reflection microscopy to record the fluctuations, the bending modulus of RBCs in isotonic condition was measured ($\approx 9 \times 10^{-19}$ Nm) [66]. Flickering spectroscopy studies of RBCs have also been used to measure membrane bending modulus [$(2.7 \pm 0.6) \times 10^{-19}$ Nm] [67].
- **Ektacytometry** It is a technique where a dilute sample of RBCs is subjected to shear flow between two transparent coaxial cylinders. The RBCs suspended in a high-viscosity medium deform into ellipsoids under the shear flow. The deformability index of RBCs can be obtained by measuring the elongation index of individual RBCs under a microscope using a rheoscope arrangement. The deformability index as a function of shear stress is studied [47, 51, 68, 69].
- **Micropore filtration** Micropore filtration was the very first throughput technique used for measuring the deformability of RBCs. It involves filtration of a dilute suspension of red blood cells through filter papers consisting of pores which are a few microns in diameter. In this technique, either RBC suspensions of a known concentration are passed through the filter paper at a constant pressure and the output concentration is obtained or the total time required for a certain volume of RBC suspension to flow through the filter paper is measured. Typically, pressure-flow curves are obtained by measuring pressure as a function of flow rate. This is then linked to the deformability of red blood cells [47, 70–73]. Micropore filtration is a high throughput experiment which can span over a range of stress regimes, depending on the exact flow conditions.
- **Microfluidic experiments** Experiments on microfluidic chips have become extremely useful in terms of mimicking in vivo conditions. The experiments can be designed for either low or high stress regimes, to assess single RBC deformability or high throughput results. Microfluidic chips with cylindrical glass capillaries of few microns have been used to study how RBCs deform under various flow rates and their recovery into normal state once they exit the narrow channel [74]. Constrictions of narrow sizes in microfluidic channel flows have been widely used to assess the deformability of RBCs [46, 47, 49, 75–77].
- **Atomic Force Microscopy (AFM)** AFM in contact mode can be used to find the Young's modulus of RBCs. Using AFM, very low forces of the order of 100 pN can be applied. The deflection curves are first obtained on a reference hard surface (glass slide), and then, on the RBC, the difference between the two curves being taken as the force-displacement curve [78, 79]. In [80], the effective Young's modulus has been measured to be 5.8 ± 0.6 kPa.
- **Nano-indentation** It is a technique used to measure the mechanical properties of materials at the nano/microscale. A probe tip (usually diamond) is used to apply load, controlled by electrical capacitance plates or magnetic coils. The load-displacement curve is obtained by pressing the indenter tip into the sample

while loading and unloading the sample [81, 82]. The study reported in [83] has found the mean reduced modulus of RBCs to be about 8.9 GPa and hardness to be 0.203.

- **Acoustophoretic orientation measurement** Acoustic flow cytometers use ultrasonically resonant capillary to combine hydrodynamic focusing with acoustic focusing to inject sample into the instrument's sheath flow. Acoustic forces are not radially symmetric, and hence, this asymmetric field is responsible for the acoustic orientation of non-spherical cells according to their intrinsic properties, such as size, density, and compressibility. Acoustic focusing of RBCs allows for high precision alignment and flow rates up to ten times greater than with conventional flow cytometers that uses only hydrodynamic focusing. This technique has been used to determine the effects of RBC storage and aging [84].
- **Artificial intelligence-based techniques** Images, and morphologic and mechanical parameters of RBCs were obtained using image algorithm and integrated data were then used as input for cloud computing to perform pathological diagnosis and quality monitoring based on a trained neural network [85]. Microfluidics technology with machine learning for clinical diagnosis [86] and assessing RBC deformability [87] have also been developed.

For the result of a technique to have any relevance to the problem of assessing the effect of altered RBC CMS on microcirculation *in vivo*, it is imperative that the method involves stress regimes that are encountered *in vivo* and is carried out on RBCs in the native state (or as close to it as possible). Of all the methods enumerated above, micropore filtration, membrane fluctuation detection, and reorientation dynamics in optical tweezers best satisfy these conditions.

7 Effect of altered RBC CMS on microcirculation

Treating RBCs extracted from an individual with no known chronic medical conditions with BSA has proved to be a reliable method of artificially altering the RBC CMS to different extents [55]. Using this technique, by varying a single parameter alone, i.e., the concentration of BSA, one can alter batches of RBCs extracted from a single source into those with varying CMS. Any difference in the results of measurements carried out on these batches of RBCs are thereby, due to the difference in the RBC CMS alone. Further, a comparison of these results with that of a study on RBCs extracted from individuals with established history of hyperglycemia [38] has established that the CMS elevation brought about artificially by BSA treatment is in the same range as the effect of this medical condition on RBC CMS. We describe here, in some detail, two studies, utilizing methods well suited to understand the effect of altered RBC CMS on microcirculation that have been carried out on RBCs where the CMS is artificially tuned with BSA treatment to the extent seen in individuals with hyperglycemia.

7.1 Reorientation dynamics in an optical tweezer

Experiments were carried out in an OT with normal RBCs and BSA treated RBCs. The method used has been described in detail in [55] and a schematic of the setup used is shown in Fig. 4.

In brief, an RBC in an optical trap that is constructed by sharply focusing a single laser beam with a Gaussian intensity profile, reorients in a manner to maximize its volume in the region of largest light intensity. This is demonstrated in the sequence of photographs shown in Fig. 5. Analysis of such videos yields a time taken by the RBC to complete the reorientation process (t_{re}) from the point of time it enters the trap with the plane of its disk perpendicular to the direction of laser beam propagation. t_{re} is found to be dependent on the laser power as well as the RBC CMS. To find a factor that scales as the RBC CMS, the excess energy (ΔE) utilized at each power to complete the reorientation process as compared to a hypothetical perfectly rigid body with identical body shape is estimated. ΔE is found to vary as a function of power, increasing initially, as seen in Fig. 6. Extrapolating from measured values of t_{re} to the power range too high to perform the experiment in without damage to the RBCs, it can be seen from Fig. 6 that ΔE finally goes to zero after going through a maximum (ΔE_{max}). This value ΔE_{max} , which is identified as the maximum energy spent on RBC membrane reformation during the process of reorientation, scales as the RBC CMS. Table 3 lists the ΔE_{max} for RBCs treated with different concentrations of BSA. It can be seen that treatment with a BSA concentration of 0.5 mg/ml leaves the RBC CMS same as that expected for RBCs from a healthy individual, while BSA concentrations higher than this render the RBCs stiffer.

7.2 Micropore filtration through pores of circular and uniform cross-section

To study the effect of altered RBC CMS on their flow through microchannels, BSA-treated RBCs were filtered through cyclopore filter papers of uniform pore diameters of $5\mu\text{m}$ (smaller than RBC diameter) and $8\mu\text{m}$ (comparable to RBC diameter) at constant volumetric flow rate using a setup whose schematic is shown in Fig. 7. From the RBC concentrations at the input and output stage of this microfiltration study, number of RBCs that pass

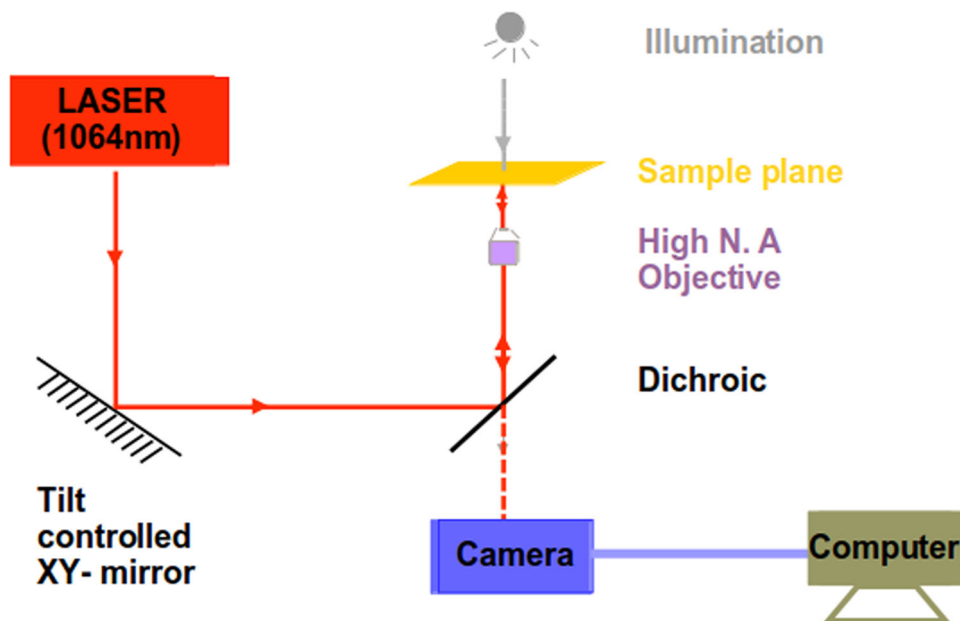


Fig. 4 Schematic of the setup for studying reorientation dynamics of RBCs in an optical trap as described in [38] and [55]

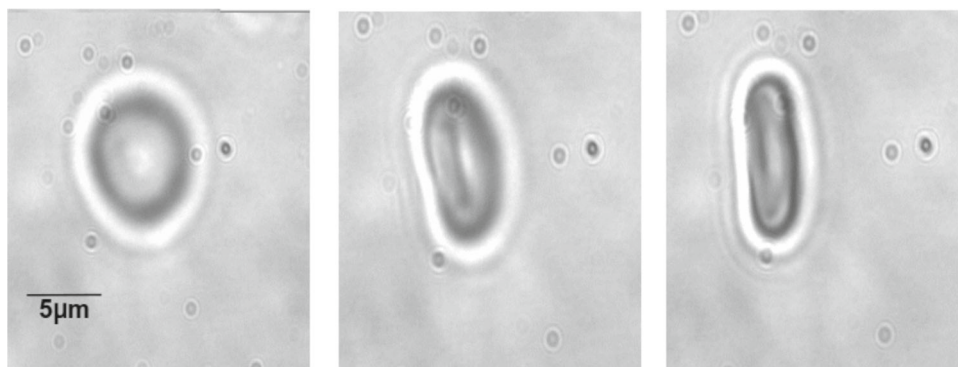


Fig. 5 Sequence of still images at 100X magnification of an RBC undergoing reorientation in an optical trap. The process is viewed along the laser propagation direction

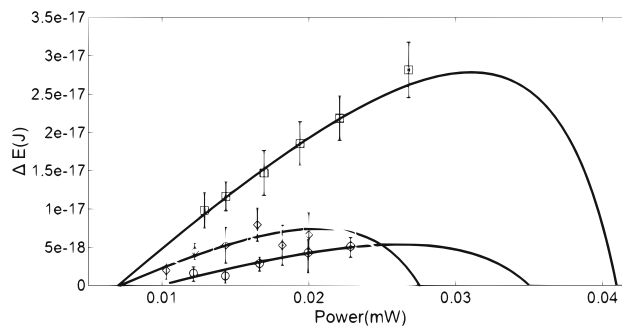
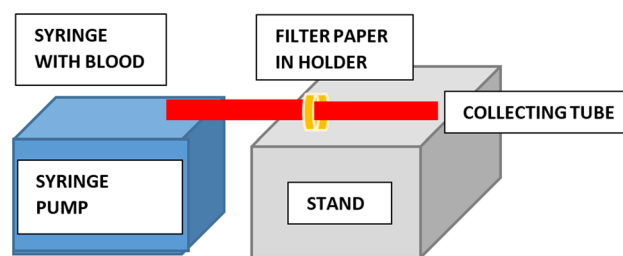


Fig. 6 Variation of excess energy ΔE with laser power for RBCs extracted from a healthy individual (normal RBCs) along with those treated with 0.5 mg/ml (diamonds), 0.1 mg/ml (circles), and 1.75 mg/ml (squares) of BSA. The symbols are the ΔE values extracted from experiments, while the continuous lines represent the extrapolated variation of ΔE even at powers not amenable to experiment [55]

Table 3 ΔE_{\max} of normal RBC along with those treated with various concentrations of BSA [55]

BSA conc.(mg/ml)	$\Delta E_{\max}(10^{-18} \text{ J})$
0.10	5.18 ± 0.91
0.35	6.42 ± 1.15
0.50	7.41 ± 1.30
0.00 (Untreated)	7.80 ± 1.50
0.70	12.97 ± 2.05
1.00	16.50 ± 1.80
1.35	23.34 ± 1.34
1.75	25.88 ± 2.10

RBCs from hyperglycemic individuals were found to have a ΔE_{\max} value of $(18.7 \pm 2.7) \times 10^{-18} \text{ J}$ [38]

**Fig. 7** Micropore filtration setup used in our lab [55]

through the filter paper per unit time per pore, N^* is obtained. The variation of N^* for the $5 \mu\text{m}$ and $8 \mu\text{m}$ pores is shown in Fig. 8. An inverse of N^* gives the average time required for one RBC to move through a pore (filtration time, T)

This study outlines a simple model to obtain the bending modulus of the RBCs from their filtration time. In brief, the filtration time is assumed to be made of two components, a time required by the RBC to deform into a suitable axisymmetric shape that can fit into the pore (T_d) and a time required for this deformed shape to pass through the length of the pore (T_p). Thus

$$T = T_d + T_p. \quad (9)$$

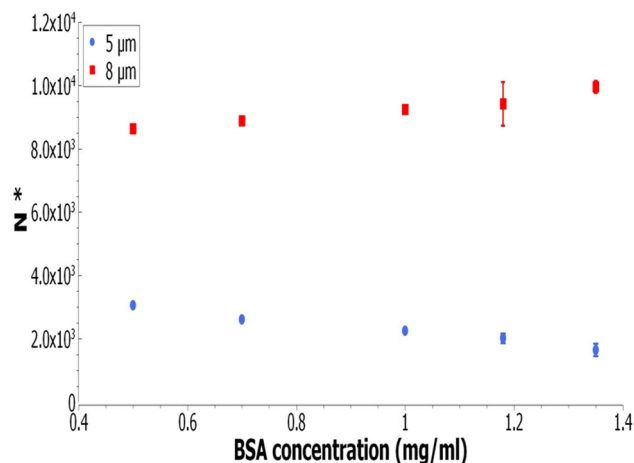
**Fig. 8** The number of RBCs that pass through a single pore in a minute (N^*) for pore diameters of $5 \mu\text{m}$ and $8 \mu\text{m}$ [55]

Table 4 Expressions used to calculate T_d and T_p

Theoretical		Experimental	
T_p	T_d	T_p	T_d
$T_p = \frac{d}{U}$ where $U = \frac{1}{K_U \beta} (K_V V - \frac{\rho V^2 a^2}{12 \eta b})$	$T_d = \frac{\epsilon_{def}}{P_{inc}}$ where $P_{inc} = \frac{1}{8} \pi \rho V_{max}^3 a^2$	d/U	$T - T_p$

d is the thickness of the filter paper; V , ρ and η are the velocity, density, and viscosity of the fluid, respectively; U is the velocity of the RBC, T is the filtration time, T_p the passage time, V_{max} the velocity of the fluid at the axial line of the channel, P_{inc} the energy incident at the RBC surface per unit time, and T_d the deformation time [55]

Table 5 x = BSA concentration used in mg/ml, filtration time (T), passage time (T_p), passage velocity (U), translational drag modification factor β , and deformation time (T_d) for flow of RBC in 8 μm and 5 μm -diameter channels for various concentrations of BSA used [55]

x	8 μm			5 μm			
	$T = T_p$ (ms)	U (mm/s)	β	T (ms)	U (mm/s)	T_p (ms)	T_d (ms)
0.50	6.94	1.44 \pm 0.03	2.02 \pm 0.03	19.60	1.00 \pm 0.02	12.00	7.60 \pm 0.40
0.70	6.75	1.48 \pm 0.11	1.96 \pm 0.15	22.99	1.02 \pm 0.17	11.67	11.32 \pm 2.00
1.00	6.47	1.54 \pm 0.01	1.88 \pm 0.02	29.41	1.07 \pm 0.02	11.21	18.20 \pm 0.30
1.18	6.34	1.57 \pm 0.11	1.84 \pm 0.13	32.51	1.09 \pm 0.14	10.95	21.56 \pm 1.50
1.35	6.02	1.65 \pm 0.03	1.75 \pm 0.03	36.44	1.15 \pm 0.03	10.41	26.03 \pm 0.40

The model in this study utilizes a constraint of constant surface area for the deformation of the RBC and estimates the energy required for such a deformation using the Helfrich elastic energy [88]

$$\epsilon_{def} = \int \frac{1}{2} E_b (2H - c_0)^2 dA, \tag{10}$$

where E_b is the RBC membrane bending modulus, and H and c_0 are the local mean and spontaneous curvatures of the RBC, respectively.

The total drag force acting on the RBC is obtained from [31] additionally including an RBC CMS-dependent translational drag factor β . The various expressions used to calculate T_p and T_d are tabulated (Table 4).

Assigning a value of $E_b = 2 \times 10^{-19} \text{Nm}$ for reported for normal RBCs [89] to the case of RBCs treated with 0.5 mg/ml BSA concentration, a value of $V_{max} = 4.27 \text{mm/s}$ is obtained. Bending moduli of the RBCs treated with other concentrations of BSA are then determined from their deformation time when filtering through the 5 μm sized pores.

From Fig. 8, it can be concluded that for pore sizes comparable to the RBC size, the filtration number (N^*) increases with increase in BSA concentration used for treating the RBCs which one knows scales as the RBC CMS. Similarly, from Fig. 8, it can be concluded that for pore sizes smaller than the RBC diameter, N^* decreases with increase in the BSA concentration used. From Table 5, it can be seen, however, that irrespective of the size of the pore vis a vis the RBC diameter, the passage velocity invariably increases, leading to a shortening of the passage time T_p with increasing BSA concentration. This suggests that stiffening of RBCs reduces the translational drag on it. The increased transfer rate of RBCs through pores with diameter comparable to that of the RBC can be attributed to the twofold reason of a reduced translational drag and that no deformation is required for the RBCs to pass through it. From Table 5, it can be seen that the RBCs require more time to deform into the required shape to pass through pores of diameters smaller than their own with increase in BSA concentration used for treating them. This additional T_d reduces the transfer rate of RBCs despite the increase in the passage velocity. The bending modulus E_b values extracted are found to vary linearly with the BSA concentration used for the treatment of RBCs for the range of concentrations used in this study (Fig. 9).

Finally, a linear correlation between the parameters ΔE_{max} and E_b that are generated by the two different studies is found (Fig. 10). Such a correlation between these two disparate methods could only be achieved, because both methods utilized identical means of artificially elevating the RBC CMS of normal RBCs.

Given this, it is now possible to give a quantitative estimate to the bending modulus for RBCs for which only reorientation dynamics in an OT have been studied. Thus for the RBCs from hyperglycemic individuals

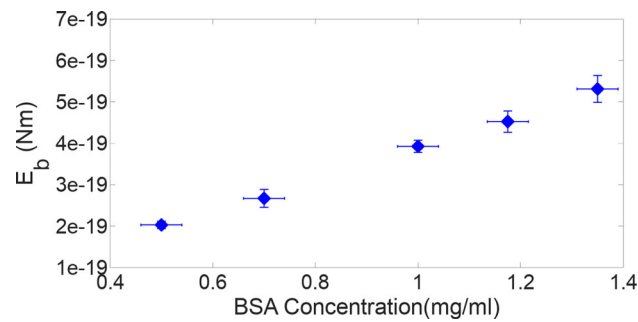


Fig. 9 Variation of E_b with BSA concentration used as reported in [55]

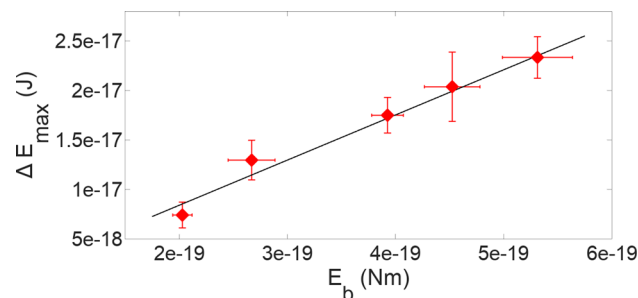


Fig. 10 Plot of ΔE_{\max} (obtained from OT) vs bending modulus E_b showing a linear correlation [55]

with ΔE_{\max} value of $(18.7 \pm 2.7) \times 10^{-18} J$ as reported in [38], one can attribute a bending modulus of about $4 \times 10^{-19} Nm$, twice that is obtained for normal RBC.

8 Conclusions

The idea behind this review was to familiarize the readers with the various experimental techniques available to gauge mechanical properties of the human red blood cell and the importance of doing so. Several commonly prevalent disease conditions affect the cell membrane properties of the red blood cell. As this is bound to affect the RBC transport in vivo especially in the capillary beds, there are bound to be consequences in terms of oxygen and nutrient supply to the tissues as well as carbon dioxide regulation. This review thereby also highlights those techniques where the stress regimes the RBCs are subjected to are close to those experienced by RBCs in vivo. The measurements made with these techniques are thereby the most relevant in the understanding of in vivo microcirculation of RBCs. Further, this review also outlines certain artificial means of altering the cell membrane stiffness of RBCs. It highlights the usefulness of such a technique in being able to establish correlations in the measurements of mechanical properties of RBCs made by two different methods with highly different throughputs.

Translation of the results of the various techniques outlined in this review to understand actual in vivo conditions requires that one overcomes several challenges. Most techniques described here work only with strongly diluted RBC samples, whereas the actual in vivo hematocrit is 40–45%. While pores of uniform diameters make the analysis of the micropore filtration experiment described here in this review, relatively simple, this is far from the actual complexity of blood flow through human vasculature. While it is difficult to analyze the results of RBC flow through complex porous material like cellulose acetate filter paper, it needs to be attempted as it is a closer approximation to the microcirculation in vivo. There are also factors that control flow rates in the capillary bed in vivo. It is important thereby to develop techniques and protocols that handle these complexities, so that one can better use the methods meant to gauge the mechanical properties to understand complications arising out of medical conditions that affect the microcirculation of RBCs.

Author contributions

Both authors have contributed equally to this work.

Funding Not applicable.

Data availability Not applicable.

Declarations

Conflict of interest There is no conflict of interest.

Ethics approval Not applicable.

Consent to participate Not applicable.

Consent for publication Obtained.

Code availability Not applicable.

References

1. S.A. Pandit et al., *Soft Matter, Volume 4: Lipid Bilayers and Red Blood Cells*, vol. 4 (Wiley - VCH, 2008)
2. R.N. Pittman, *Regulation of Tissue Oxygenation* (Morgan and Claypool Life Sciences, San Rafael, 2011)
3. J.A. Blom, *Monitoring of Respiration and Circulation* (CRC Press, 2003)
4. B.N. Alamri et al., Hyperglycemia effect on red blood cells indices. *Eur. Rev. Med. Pharmacol. Sci.* **23**, 2139 (2019)
5. M. Singh, M. Kumravel, Influence of jaundice on aggregation process and deformability of erythrocytes. *Clin. Hemorheol. Microcirc.* **15**(3), 273 (1995)
6. J. Rey, P.A. Buffet, L. Ciceron, G. Milon, O. Mercereau-Puijalon, I. Safeukui, Reduced erythrocyte deformability associated with hypoargininemia during plasmodium falciparum malaria. *Sci. Rep.* **4**, 3767 (2014)
7. Y. Alapan, J.A Little, U.A. Gurkan, Heterogeneous red blood cell adhesion and deformability in sickle cell disease. *Sci. Rep.* **4**, 7173 (2014)
8. BCOpentext: anatomy and physiology: the cardiovascular system: blood vessels and circulation, (Ch18). Chap. 20. <https://opentextbc.ca/anatomyandphysiology/chapter/20-1-structure-and-function-of-blood-vessels/>. Accessed May 2020
9. T.M.C. Abbott et al., Dark energy survey year 1 results: constraints on extended cosmological models from galaxy clustering and weak lensing. *Phys. Rev. D* **99**(12), 123505 (2019). <https://doi.org/10.1103/PhysRevD.99.123505>. arXiv: [1810.02499](https://arxiv.org/abs/1810.02499) [astro-ph.CO]
10. L. Lanotte, J.C. Mauer, D.A. Fedosov et al., Red cells dynamic morphologies govern blood shear thinning under microcirculatory flow conditions. *PNAS* **113**(50), 13289 (2016)
11. G.J. Tortora, B. Derrickson, *Introduction to the Human Body: The Essentials of Anatomy and Physiology*, 8th edn. (John Wiley and Sons, Inc. 2010)
12. F. Violi, R. Marino, M.T. Milite, L. Loffredo, Nitric oxide and its role in lipid peroxidation. *Diabetes Metab. Res. Rev.* **15**(4), 283 (1999)
13. V. Kuhn et al., Red blood cell function and dysfunction: Redox regulation, nitric oxide metabolism, anemia. *Antioxid. Redox Signal.* **26**(13), 718 (2017)
14. S. Oliveira, C. Saldanha, An overview about erythrocyte membrane. *Clin. Hemorheol. Microcirc.* **44**, 63 (2010)
15. K.A. Brown, Erythrocyte metabolism and enzyme defects. *Lab. Med.* **27**(5), 329–333 (1996)
16. J.L.V. Corrons, L.B. Casafont, E.F. Frasnado, Concise review: how do red blood cells born, live, and die? *Ann. Hematol.* **100**(10), 2425–2433 (2021)
17. D. Drenckhahn, in *Blood Cells, Rheology, and Aging*, ed. by D. Platt. Removal of Old and Abnormal Red Blood Cells from Circulation: Mechanical and Immunologic Mechanisms (Springer, Berlin, Heidelberg, 1988), pp. 62–72. https://doi.org/10.1007/978-3-642-71790-1_7
18. I.V. Pivkina, Z. Pengc, G.E. Karniadakise, P.A.B.M. Daod, S. Suresh, Biomechanics of red blood cells in human spleen and consequences for physiology and disease. *Proc. Natl. Acad. Sci.* **113**(8), 7804–7809 (2016)
19. R.E. Mebius, G. Kraal, Structure and function of the spleen. *Nat. Rev. Immunol.* **5**, 606–616 (2005)
20. G. Tomaiuolo, Biomechanical properties of red blood cells in health and disease towards microfluidics. *Biomicrofluidics* **8**, 051501 (2014)
21. K. Jeongho, L. HoYoon, S. Sehyun, Advances in the measurement of red blood cell deformability: a brief review article. *J. Cell. Biotechnol.* **1**(1), 63 (2015)
22. V.T. Marchesi, The relevance of research on red cell membranes to the understanding of complex human disease: A personal perspective. *Annu. Rev. Pathol. Mech. Dis.* **3**, 1 (2008)
23. K. Khairy, J. Foo, J. Howard, Shapes of red blood cells: comparison of 3d confocal images with the bilayer - couple model. *Cell. Mol. Bioeng.* **1**, 173 (2008)
24. B.F. Rodak, E.M. Keoghane, G.A. Fritsma (eds.), in *Clinical Principles and Applications*, 6th edn. Chap 6. Erythrocyte Metabolism and Membrane Structure and Function Hematology (Elsevier Health Sciences, 2019). https://doi.org/10.1007/978-3-642-71790-1_7

25. T. Fujimoto, I. Parmryd, Interleaflet coupling, pinning, and leaflet asymmetry-major players in plasma membrane nanodomain formation. *Front. Cell Dev. Biol* **10**, 155 (2017)
26. R.P. Chhabra, *Non-Newtonian Fluids: An Introduction in Rheology of Complex Fluids* (Springer-Verlag, New York, 2010), p.3
27. W.Y. Chan, Y. Ding, J.Y. Tu, Modeling of non-Newtonian blood flow through a stenosed artery incorporating fluid-structure interaction. *ANZIAM* **47**, 507 (2007)
28. M. A. Jamalabadi, M. Daqiqshirazi, H. Nasiri, M.R. Safaei, T.K. Nguyen, *PLoS One* **13**(2), e0192138 (2018)
29. S.A. Bereger, L.D. Jou, Flows in stenotic vessels. *Annu. Rev. Fluid Mech.* **32**, 347 (2002)
30. D.N. Ku, Blood flow in arteries. *Annu. Rev. Fluid Mech.* **29**, 399 (1997)
31. T.C. Chen, R. Skalak, Stokes flow in a cylindrical tube containing a line of spheroidal particles. *Appl. Sci. Res.* **22**, 403 (1970)
32. N. Babu, Influence of hypercholesterolemia on deformability and shape parameters of erythrocytes in hyperglycemic subjects. *Clin. Hemorheol. Microcirc.* **41**(3), 169 (2009)
33. C.S. Lau, A.R. Saniabadi, J.J.F. Belch, Reduced red blood cell deformability in patients with rheumatoid vasculitis. *Arthritis Rheumatol.* **38**, 248 (1995)
34. A.K. Saha, B.R. Schmidt, J. Wilhelmy, V. Nguyena, A. Abugherira et al., Red blood cell deformability is diminished in patients with chronic fatigue syndrome. *Clin. Hemorheol. Microcirc.* **1**, 1 (2018)
35. N. Babu, M. Singh, Influence of hyperglycemia on aggregation, deformability and shape parameters of erythrocytes. *Clin. Hemorheol.* **31**, 273 (2004)
36. K. Tsukada, E. Sekizuka, C. Oshio, H. Minamitani, Direct measurement of erythrocyte deformability in diabetes mellitus with a transparent microchannel capillarymodel and high- speed video camera system. *Microvasc. Res.* **61**, 231 (2001)
37. J.S. Moon et al., Impaired rbc deformability is associated with diabetic retinopathy in patients with type 2 diabetes. *Diabetes Metab.* **42**(6), 448 (2016)
38. P. Parthasarathi et al., Orientational dynamics of human red blood cells in an optical trap. *J. Biomed. Opt.* **18**(2), 025001 (2013)
39. S.K. Jain, Hyperglycemia can cause membrane lipid peroxidation and osmotic fragility in human red blood cells. *J. Biol. Chem.* **264**(35), 21340 (1989)
40. B. Cooke, N. Mohandas, R. Coppel, Malaria and the red blood cell membrane. *Semin. Hematol.* **41**(2), 173 (2004)
41. J.G.G. Dobbe et al., Analyzing red blood cell deformability distributions. *Blood Cells Mol. Dis.* **28**(3), 373 (2002)
42. S. Eber, S.E. Lux, Hereditary spherocytosis-defects in proteins that connect the membrane skeleton to the lipid bilayer. *Semin. Hematol.* **41**(2), 118 (2004)
43. T. Gomi, T. Ikeda, F. Ikegami, Beneficial effect of a β -blocker on hemorheology in patients with essential hypertension. *AJH* **10**, 886 (1997)
44. M. Grau et al., Even patients with mild covid-19 symptoms after sars-cov-2 infection show prolonged altered red blood cell morphology and rheological parameters. *J. Cell Mol. Med.* **26**(10), 3022–3030 (2022)
45. H.M. Al-Kuraishy, O.H.E.-S.B.G. Al-Gareeb AI: Covid-19 and erythrocrine function: The roller coaster and danger. *Int. J. Immunopathol. Pharmacol.* **36**, 3946320221103151 (2022)
46. Y. Zheng, J. Nguyen, C. Wang, Y. Sun, Electrical measurement of red blood cell deformability on a microfluidic device. *Lab Chip* **13**, 3275 (2013)
47. J.M. Sosa, N.D. Nielsen, S.M. Vignes, T.G. Chen, S.S. Shevkoplyas, The relationship between red blood cell deformability metrics and perfusion of an artificial microvascular network. *Clin. Hemorheol. Microcirc.* **57**(3), 275 (2014)
48. B.B. Gupta, V. Seshadri, Flow of hardened red blood cell suspensions through narrow tubes. *Microvasc. Res.* **17**, 263 (1979)
49. A.M. Forsyth, J. Wan, W.D. Ristenpart, H.A. Stone, The dynamic behavior of chemically “stiffened” red blood cells in microchannel flows. *Microvasc. Res.* **80**, 37 (2010)
50. J. Barbee, Concentration reduction and dilatant flow behavior in suspensions of hardened human red cells. *Trans. Soc. Rheol.* **17**, 413 (1973)
51. O.K. Baskurt et al., Comparison of three commercially available ektacytometers with different shearing geometries. *Biorheology* **46**, 251 (2009)
52. H. Lim, S.M. Back, J. Nam, H. Choi, Determination of red blood cell deformability using centrifugal force in a three-dimensional-printed mini-disk (3d-pmd). *PLoS One* **13**(5), e0197619 (2018)
53. A. Williams, The effect of bovine and human serum albumins on the mechanical properties of human erythrocyte membranes. *Biochim. Biophys. Acta* **307**, 58 (1973)
54. A. Jay, Geometry of the human erythrocyte-i. Effect of albumin on cell geometry. *Biophys. J.* **15**, 205 (1975)
55. R. Selvan, P. Parthasarathi, S.S. Iyengar, S. Ananthamurthy, S. Bhattacharya, Estimation of membrane bending modulus of stiffness tuned human red blood cells from micropore filtration studies. *PLoS One* **14**(12), 1–20 (2020). <https://doi.org/10.1371/journal.pone.0226640>
56. C. Dupuy-Fons, J.-F.D.-Z. Brun, C. Mallart, J. Carvajal, M.L. Fussellier, L.B.A. Orsetti, In vitro influence of zinc and magnesium on the deformability of red blood cells artificially hardened by heating. *Biol* **47**, 247 (1995)
57. F.K. Glenister, R.L. Coppel, A.F. Cowman, N. Mohandas, B.M. Cooke, Contribution of parasite proteins to altered mechanical properties of malaria-infected red blood cells. *Blood* **99**, 1060 (2002)
58. E.A. Evans, Bending elastic modulus of red blood cell membrane derived from buckling instability in micropipet aspiration tests. *Biophys. J.* **43**(1), 27 (1983)

59. S. Chen, K.L. Paul, R. Skalak, S. Usami, A. Tözeren, Theoretical and experimental studies on viscoelastic properties of erythrocyte membrane. *Biophys. J.* **24**(2), 463 (1978)
60. T. Barnes, A. Shulman, A. Farone, M. Farone, D. Erenso, Assessment of the elasticity of erythrocytes in different physiological fluids by laser traps. *OPJ* **3**, 211 (2013)
61. R. Agarwal et al., Assessment of red blood cell deformability in type 2 diabetes mellitus and diabetic retinopathy by dual optical tweezers stretching technique. *Sci. Rep.* **6**, 15873 (2016)
62. A. Paul, R. Pallavi, U.S. Tatu, V. Natarajan, The bystander effect in optically trapped red blood cells due to plasmodium falciparum infection. *Trans. R. Soc. Trop. Med. Hygiene* **107**(4), 220–223 (2013)
63. T. Yang, F. Bragheri, P.A. Minzioni, A comprehensive review of optical stretcher for cell mechanical characterization at single-cell level. *Micromachines* **7**(5), 90 (2016)
64. J. Guck et al., The optical stretcher: a novel laser tool to micromanipulate cells. *Biophys. J.* **81**, 767 (2001)
65. Y. Alster, A. Loewenstein, S. Levin, M. Lazar, R. Korenstein, Low-frequency submicron fluctuations of red blood cells in diabetic retinopathy. *Arch. Ophthalmol.* **116**(10), 1321 (1998)
66. J. Evans, W. Gratzler, N. Mohandas, K. Parker, J. Sleep, Fluctuations of the red blood cell membrane: relation to mechanical properties and lack of atp dependence. *Biophys. J.* **94**(10), 4134 (2008)
67. R.R. Garcia, I.L. Montero, M. Mell, G. Egea, N.S. Gov, F. Monroy, Direct cytoskeleton forces cause membrane softening in red blood cells. *Biophys. J.* **108**, 2794 (2015)
68. M. Rabai, J.A. Detterich, R.B. Wenby, T.M. Hernandez, K. Toth, H.J. Meiselman, J.C. Wood, Deformability analysis of sickle blood using ektacytometry. *Biorheology* **51**, 159 (2014)
69. G.J. Streekstra, J.G.G. Dobbe, A.G. Hoekstra, Quantification of the fraction poorly deformable red blood cells using ektacytometry. *Opt. Exp.* **18**(13), 14173 (2010)
70. M. Moia, A. Tripodi, E. Mozzi, D. Mari, P.M. Mannucci, An improved method for measuring red blood cell filterability. *Ric Clin. Lab.* **15**(2), 127 (1985)
71. C.D. Brown, S.H. Ghali, Z. Zhao, L.L. Thomas, E.A. Friedman, Association of reduced red blood cell deformability and diabetic nephropathy. *Kidney Int.* **67**, 295 (2005)
72. U.J. Kirkpatrick, R.A. Adams, A. Lardi, C.N. McCollum, Rheological properties and function of blood cells in stored bank blood and salvaged blood. *Br. J. Haematol.* **101**, 364 (1998)
73. S. Shin, Y. Ku, N. Babu, M. Singh, Erythrocyte deformability and its variation in diabetes mellitus. *Indian J. Exp. Biol.* **45**, 121 (2007)
74. G. Tomaiuolo, M. Simeone, V. Martinelli, B. Rotoli, S. Guido, Red blood cell deformation in micro - confined flow. *Soft Matter* **5**, 3736 (2009)
75. M. Faivre, M. Abkarian, K. Bickraj, H.A. Stone, Geometrical focusing of cells in a microfluidic device: An approach to separate blood plasma. *Biorheology* **43**, 147 (2006)
76. X. Deng, S.P. Duffy, M.-E. Myrand-Lapierre, K. Matthews, A.T. Santoso, Y.-L. Du, K.S. Ryan, H. Ma, Reduced deformability of parasitized red blood cells as a biomarker for anti-malarial drug efficacy. *Malar. J.* **14**, 428 (2015)
77. D. Bento, R.O. Rodrigues, V. Faustino, D. Pinho, C.S. Fernandes, A.I. Pereira, V. Garcia, J.M. Miranda, R. Lima, Deformation of red blood cells, air bubbles, and droplets in microfluidic devices: Flow visualizations and measurements. *Micromachines* **9**(4), 151 (2018)
78. I. Dulińska et al., Stiffness of normal and pathological erythrocytes studied by means of atomic force microscopy. *J. Biochem. Biophys. Methods* **66**, 1 (2006)
79. J.L. Maciaszek, G. Lykotrafitis, Sick cell trait human erythrocytes are significantly stiffer than normal. *J. Biomech.* **44**, 657 (2011)
80. M. Lekka, M. Fornal, G. Pyka-Fosciak, K. Lebed, B. Wizner, T. Grodzicki, J. Styczen, Erythrocyte stiffness probed using atomic force microscope. *Biorheology* **42**, 307 (2005)
81. C.A. Schuh, Nanoindentation studies of materials. *Mater. Today* **9**(5), 32 (2006)
82. J. Chen, Nanobiomechanics of living cells: a review. *Interface Focus* **4**, 20130055 (2014)
83. Z. Yong et al., Experimental and fem study of effect of smoking on red blood cells. *Int. J. Biol. Eng.* **5**(1), 16 (2015)
84. G. Rico, J. Juncà, M.D. Ward, J.A. Bradford, J. Bardina, J. Petriz, Acoustophoretic orientation of red blood cells for diagnosis of red cell health and pathology. *Sci. Rep.* **8**, 15705 (2018)
85. Y.L. Longfei Chen et al., Touchable cell biophysics property recognition platforms enable multifunctional blood smart health care. *Microsystems and Nanoengineering* **7**(103), 13553 (2021)
86. A.M. Valeria Rizzuto et al., Combining microfluidics with machine learning algorithms for RBC classification in rare hereditary hemolytic anemia. *Sci. Rep.* **11**, 13553 (2021). <https://doi.org/10.1038/s41598-021-92747-2>
87. E.S. Lamoureux, E. Islamzada, M.V.J. Wiens, K. Matthews, S.P. Duffy, H. Ma, Assessing red blood cell deformability from microscopy images using deep learning. *Lab. Chip* **22**, 26–39 (2022). <https://doi.org/10.1039/D1LC01006A>
88. S. Munoz, J.L. Sebastián, M. Sancho et al., Elastic energy of the discocyte- stomatocyte transformation. *BBA* **1838**(3), 950 (2014)
89. J. Zhang, P.C. Johnson, A.S. Popel, Effects of erythrocyte deformability and aggregation on the cell free layer and apparent viscosity of microscopic blood flows. *Microvasc. Res.* **77**(3), 265 (2009)

Springer Nature or its licensor (e.g. a society or other partner) holds exclusive rights to this article under a publishing agreement with the author(s) or other rightsholder(s); author self-archiving of the accepted manuscript version of this article is solely governed by the terms of such publishing agreement and applicable law.